IEEE Photonics Journal
An IEEE Photonics Society Publication

Open Access

Underwater Imaging Based on LF and Polarization

Volume 11, Number 1, February 2019

Yu Tian
Bin Liu
Xinyan Su
Lipeng Wang
Ke Li

DOI: 10.1109/JPHOT.2018.2890286
1943-0655

IEEE photonics SOCIETY

IEEE

Underwater Imaging Based on LF and Polarization

Yu Tian,[1,2] **Bin Liu**,[1,2] **Xinyan Su**,[1,2] **Lipeng Wang**,[1,2] **and Ke Li**[1,2]

[1]School of Information and Communication Engineering, North University of China, Taiyuan 030051, China
[2]National Defense Technology Key Laboratory of Electronic Testing Technology, Taiyuan 030051, China

DOI:10.1109/JPHOT.2018.2890286

Manuscript received October 9, 2018; revised December 17, 2018; accepted December 26, 2018. Date of publication January 1, 2019; date of current version January 11, 2019. This work was supported in part by the National Defense Science and Technology Key Laboratory of Electronic Testing Technology under Grant 614200010401. Corresponding author: Yu Tian (e-mail: laipiadou@163.com).

Abstract: The underwater image restoration based on polarization information has achieved good results in improving the image quality in scattering media. However, the previous methods are difficult to obtain the true distribution of degree of polarization in the scene. In this paper, we combine synthetic aperture imaging with polarimetric imaging, and propose a method for retrieving radiation of object based on the degree of polarization and intensity of backscattering at the multi-view image. In addition, compared with the previous methods, the proposed method can achieve simultaneous acquisition of four-dimensional light field information and polarization information, effectively increasing the information dimension obtained by single imaging. In order to verify the effectiveness and superiority of the proposed method, we have established a relevant experimental platform and compared with the experimental results of the previous methods, and obtained the expected experimental results.

Index Terms: Synthetic aperture imaging, polarimetric imaging, underwater image restoration.

1. Introduction

The image quality in turbid media may be limited, because the reflected light of the target scene is partially absorbed by the turbid medium, at the same time, some undesired light scattered into the optical path [1]. Both of these two effects can adversely affect the quality in the underwater imaging. However, underwater imaging is of great significance in practice [2], [3]. Consequently, in order to eliminate such negative effects and enhance the quality of the underwater images, many dehazing methods have been proposed, and some of them are really effective [4]–[9].

There are many representative methods for underwater image restoration, such as: dark channel prior [5], confocal imaging [10], [11], self-tuning restoration filter [12], and so on. In particular, the polarimetric imaging method proposed by Schechner in 2001 is considered to be an effective method for recovering the image in scattering medium [6]. However, this assumption may not be suitable for all situations in practice. The previous work of polarimetric imaging in turbid media typically defines the degree of polarization(DOP) of backscatter and the backscattering intensity at different locations of the image as a space constant [13], or uses local information in the image to fit the global backscattering intensity and the degree of polarization of backscatter [15]. However, in

particular, the degree of polarization is different at different spatial viewing angles. Especially, in the case of active illumination, a non-uniform light field is generated in the water, which is even more dramatic, and thus there could be significant errors in the recovered image [16].

In this paper, we focus on the variation of the degree of polarization of backscattering in space during underwater imaging. We analyzed the limitations of previous polarization-based underwater image restoration methods, proposed a method for estimating the spatial distribution of DOP of the backscatter and the irradiance of backscatter at infinity based on synthetic aperture imaging techniques. We built an experimental environment and carried out practical experiments of multiple sets of polarimetric underwater imaging to prove the feasibility and superiority of the proposed method.

This article is described in the following sections: Section 2 presents prior work, Section 3 details our technical methods, and Section 4 describes the experimental setup and experimental results. Finally, Sections 5 and 6 analyze and discuss the experimental results and give recommendations for future work.

2. Related Work

In recent years, polarized underwater imaging technology has been well developed, by considering the polarization state of transmitted or backscattered light, the visibility of the image can be effectively improved.

In 2001, Schechner *et al.* first proposed the use of polar imaging to improve the quality of images taken in foggy days. In the following years, his team further refined this theory, in 2009, they completed the underwater experiment of polarimetric imaging and achieved pretty good experimental results [6], [16].

Xu *et al.* analyzed the degree of polarization attenuation during underwater light transmission, and evaluated the performance of polarized underwater imaging [14].

Hu *et al.* proposed a method for recovering the underwater image based on the transmittance correction, which transforms the transmittance for the low depolarized objects from negative values to the positive values that optimize the image quality with a simple algorithm of polynomial fitting [13].

In 2018, Hu *et al.* proposed a method of retrieving the objects radiance based on estimating the degree of polarization and the intensity of backscatter at different positions of the image [15].

However, previous work of underwater polarimetric imaging typically assumed that the degree of polarization of the backscatter and the intensity of backscattering at different locations of the image are constants in space, or that the global backscattering intensity and the degree of polarization of backscattering are fitted using local information in the image.

In practice, there are many factors that affect the degree of polarization of backscatter and the intensity of backscatter, so whether you assume them as a constant or a local distribution to fit the global situation, it does not reflect the real situation. A typical example, in an underwater active light illumination environment, a non-uniform light field is generated due to the influence of illumination. In this case, the intrinsic parameters of the underwater imaging conditions will vary with the viewing angle changes.

In recent years, with the development of computational imaging theory, light field imaging has begun to be used in the field of underwater imaging. K.Skinner *et al.* has previously proposed a method for 3D reconstruction of underwater scenes with a light field camera, but this method was tested in pure water [17]. A. Skinner *et al.* used the Lytro first-generation light field camera for underwater imaging, and then used the Dark Channel Prior algorithm to dehaze the sub-images [18]. Tian *et al.* present a new single image restoration algorithm, and apply it to each view in the light field, to recover a single image of higher quality than what is possible from a single view [19].

The use of light field imaging in the underwater imaging process can achieve the acquisition of 4D light field information in one imaging process, which effectively increases the amount of information of the image. However, Previous studies typically use the single light field camera for photography and then use a single frame image dehazing algorithm for image recovery. Although it has been

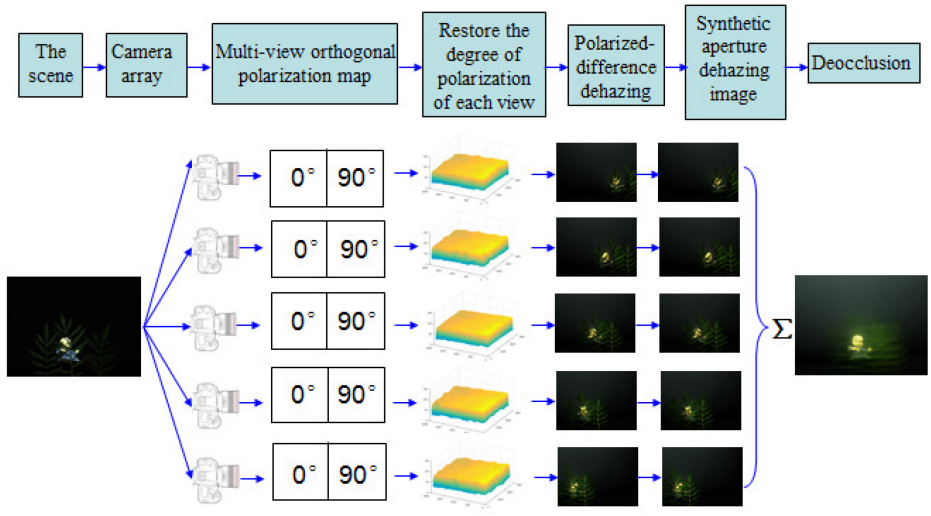

Fig. 1. Algorithm workflow.

proven to be superior to conventional underwater imaging methods, there are still some limitations. On the one hand, the existing light field camera has a small aperture and low resolution, resulting in a small field of view and low resolution of the restored image; on the other hand, the image restoration algorithm is not suitable for real-time processing because of the time-consuming of de-hazing processing, and the prior knowledge or premise assumptions involved in the technology are mostly limited,which makes the application scope of the technology limited.

3. Optical Models of Underwater Imaging

The framework of the proposed algorithm is displayed in Fig. 1. Synthetic aperture imaging acquires 4D light field information by acquiring the target images at different viewing angles by linear arrangement of multiple cameras. We can obtaine two sets of multi-view images with orthogonal polarization states by placing a linear polarizer in front of each camera and imaging in two orthogonal polarization states by rotating a linear polarizer. The polarization information and the 4D information of the light field are completely recorded, which can be expressed as $L_{\parallel}$(u, v, s, t) and $L_{\perp}$(u, v, s, t), where u,v indicates that the camera array consists of u $\times$ v cameras, and s, t indicates that the image resolution of each camera is $s \times t$. Using these two sets of images, each sub-aperture image is first dehazed, and then the synthetic aperture algorithm is used to optimize the defogging and deocclusion.

3.1 Subaperture Image Dehazing Algorithm

We will begin with a basic model of polarized-difference dehazing in terrestrial applications and describe an extended model of underwater dehazing for multi-view images of the light field [20]. The total intensity of each subaperture image of the synthetic aperture is an incoherent superposition of the direct transmitted light intensity and the backscattered light intensity. The target transmitted light D(u, v, s, t) and the intensity of backscattered light B(u, v, s, t) can expressed as:

$$\begin{aligned} D(u, v, s, t) &= \mathrm{L}'(u, v, s, t)\mathrm{t}(u, v, s, t) \\ B(u, v, s, t) &= \mathrm{A}_{\infty}[1 - \mathrm{t}(u, v, s, t)] \end{aligned} \tag{1}$$

Where L'(u, v, s, t) indicates the restored image, A_{∞} corresponds to the intensity of backscatter, t(u, v, s, t) represents the light transmission transmittance in the water.

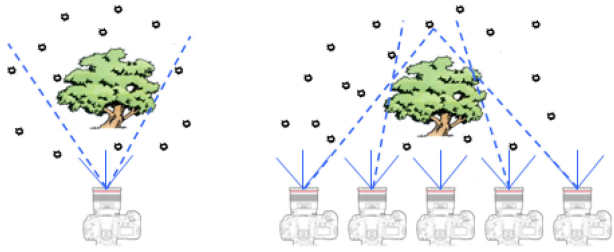

(a) (b)

Fig. 2. (a) The amount of information captured in the traditional way is limited by the field of view. (b) The camera array has a larger field of view, which can detect occluded areas and enrich the amount of information acquired.

So the each subaperture image with orthogonal polarization states $L_{\parallel}(u, v, s, t)$ and $L_{\perp}(u, v, s, t)$ can be expressed as:

$$\begin{aligned} L_{\parallel}(u, v, s, t) &= D_{\parallel}(u, v, s, t) + B_{\parallel}(u, v, s, t) \\ L_{\perp}(u, v, s, t) &= D_{\perp}(u, v, s, t) + B_{\perp}(u, v, s, t) \end{aligned} \tag{2}$$

The degree of polarization of backscattering at any viewing angle can be expressed as:

$$P_{scat}(u, v, s, t) = \frac{B_{\parallel}(u, v, s, t) - B_{\perp}(u, v, s, t)}{B_{\parallel}(u, v, s, t) + B_{\perp}(u, v, s, t)} = \frac{\Delta B(u, v, s, t)}{B(u, v, s, t)} \tag{3}$$

Combining equations (1), (2), and (3), the transmittance is expressed as:

$$t(u, v, s, t) = 1 - \frac{\Delta B(u, v, s, t)}{P_{scat} A_{\infty}} \tag{4}$$

Similar to the calculation process of ΔB, ΔD is expressed as:

$$\Delta D = D_{\parallel}(u, v, s, t) - D_{\perp}(u, v, s, t) \tag{5}$$

In previews works [6], [13], the polarization of the object radiance is ignored. So, here we define the value of ΔD as 0. In this case, ΔB can be expressed as:

$$\Delta B(u, v, s, t) = L_{\parallel}(u, v, s, t) - L_{\perp}(u, v, s, t) = \Delta L(u, v, s, t) \tag{6}$$

According to the equations above,the restored sub-aperture image expression $L'(u, v, s, t)$ can be deduced as:

$$L'(u, v, s, t) = \frac{L_{\parallel}(u, v, s, t) + L_{\perp}(u, v, s, t) - A_{\infty}[1 - t(u, v, s, t)]}{t(u, v, s, t)} \tag{7}$$

In order to acquire the object irradiance $L'(u, v, s, t)$ according to the algorithm in (4) and (7), a major problem is to estimate the values of A_{∞} as well as the DOP of backscatter P_{scat}.

3.2 Estimating the Spatial Distribution of A_{∞} and P_{scat}

In the process of solving P_{scat} and A_{∞} in the traditional method, since its image acquisition process is limited by the field of view,it is generally considered that the values of P_{scat} and A_{∞} are constants, which are global parameters across the whole field of view [20], [21]. In this paper, we use synthetic aperture for image acquisition, because of its larger field of view, we can capture information that is not available in traditional imaging methods, getting the global information [22], see Fig. 2. The multi-view image acquired by the synthetic aperture is used to fill the distribution of P_{scat} and A_{∞} in the target area, and the global distribution of P_{scat} and A_{∞} is obtained. In this way, the radiance of

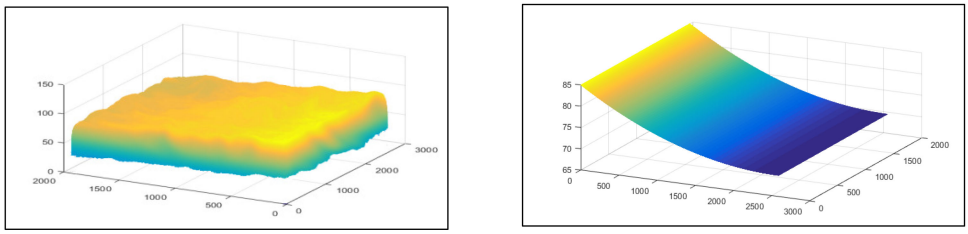

(a) (b)

Fig. 3. (a) The spatial distribution of the degree of polarization of backscatter. (b) Fit results of the degree of polarization of backscatter.

the restored sub-aperture image can be expressed as:

$$L'(u, v, s, t) = \frac{L_{\parallel}(u, v, s, t) + L_{\perp}(u, v, s, t) - \frac{\Delta L(u,v,s,t)}{\omega * P_{scat}}}{1 - \frac{\Delta L(u,v,s,t)}{\omega * P_{scat} A_{\infty}}} \tag{8}$$

Since we ignore the polarization of the object radiance, it may affect the experimental results, so herewe employ the parameter ω to modify P_{scat}. In our experiment, the value of ω was 1.08.

The spatial distribution of the P_{scat} is shown in Fig. 3(a), in Fig. 3(b) we show the distribution of the degree of polarization of the backscatter fitted by the method in [15]. Whether it is a fitting method or a constant replacement, the distribution of the degree of polarization of the backscattering cannot be truly reflected. The distribution of the degree of polarization of the backscatter can be more accurately described using our method. As for the solution process of A_{∞} is the same as P_{scat}, it is not described here.

3.3 Image Recovery and Foreground Occlusion Removal

After completing the above initial dehazing operation,we noticed that there is contain noise in each dehazed sub-aperture images. Using the synthetic aperture algorithm, the sub-aperture images that have completed the initial dehazing are respectively accumulated by the same field of view and then averaged to obtain a final de-haze image. This process is similar to the mean filtering, the difference is that the mean filtering is used in the plane of a single image, and we are using it in the epipolar-plane of synthetic aperture multi-view image [18]. As shown in Fig. 6, compared to the initial dehazed image the noise influence is effectively suppressed, and the image restoration effect is optimized.

We have recovered a dehazed image with improved quality compared to the initial dehazing estimate. However, in these dehazed images the foreground object obscures the target. In order to solve this problem, the synthetic aperture refocusing algorithm is used to remove the foreground occlusion [23]. In order to solve this problem, the synthetic aperture refocusing algorithm is used to remove the foreground occlusion. Focusing the synthesized virtual aperture at the target location using a refocusing algorithm, because the depth of field is very shallow, the foreground occlusion is severely weakened, and the occlusion effect can be achieved.

4. Experiment and Results

4.1 Experiment

As shown in the experimental setup, the imaging device is a color CMOS camera (MV-EM500M/C) with a pixel count of $2592 * 1944$. The camera is fixed on the displacement platform and a rotatable linear polarizer is placed in front of the camera as an analyzer. The camera array is simulated by driving the displacement platform at equal intervals to obtain light field information. In this paper, we simulated a 1×19 camera array for image acquisition. The light source is a white light LED

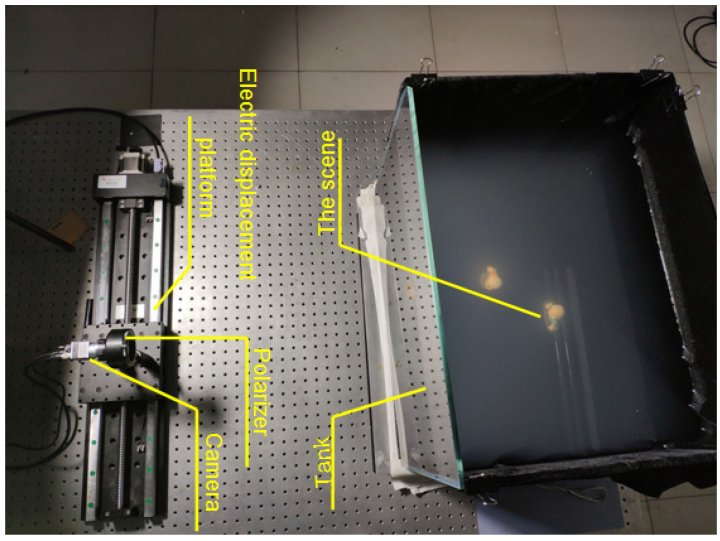

Fig. 4. The experiment system.

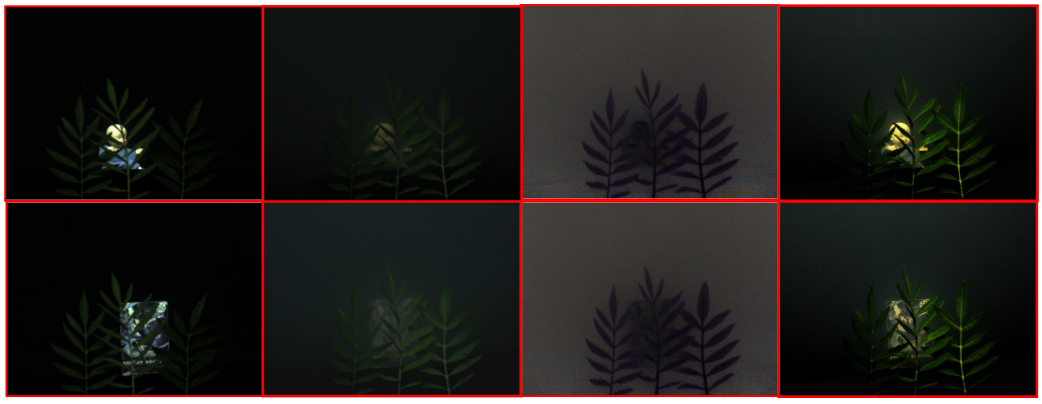

Fig. 5. From left to right: Image taken in clear water, the co-linear image, the Polarization map, recovered image by our method.

diffusing light source. A glass water tank measuring 45 cm $\times$ 65 cm $\times$ 45 cm is used, and the water tank is lined with an opaque black curtain to prevent the reflected light from the inner wall of the tank from affecting the experimental results. To simulate the backscattering conditions in water, we pour 102375 cm^3 (45 cm $*$ 65 cm $*$ 35 cm) of water into the tank, then add 80 ml of milk, mix well. The target object is placed at the end of the tank at a distance of 1 m from the camera plane.

4.2 Experimental Results

Fig. 5 shows the results of our pipeline for two target objects. Note that each light field image consists of 19 multi-view images, but only the center image of each light field image is shown here. The left image shows a high-resolution image taken in clean water for visual reference. Next is the co-linear image $L_{\parallel}(u, v, s, t)$. It display the attenuation typical of underwater images, where the haze effect dominates the image. And the next represents the Polarization map. The final image is the result of our proposed method after performing polarized-difference dehazing operation and synthesizing views. The resulting images have reduced noise and maintain the details of the imaged objects.

Fig. 6. The recovered images by different methods,from left to right: UDCP,traditional polarized-difference dehazing(PD), our polarized-difference dehazing, Synthetic aperture dehazing.

TABLE 1
Quantitative Evaluation of Experimental Results by Different Methods

Experiments	PSNR				SSIM			
	UDCP	PD	Our PD	SAD	UDCP	PD	Our PD	SAD
Fig. 4, toy monk	21.3406	21.4314	23.6426	23.7940	0.7854	0.8336	0.8449	0.8879
Fig. 4, card	21.9024	22.0696	24.0368	24.5571	0.7766	0.8211	0.8310	0.8783

In order to verify the superiority of our model, we compared the initial results of dehazing and the final dehazing results by Synthetic aperture with the results of the Underwater Dark Channel Prior (UDCP) and the experimental results of using the polarization difference method described in [15], we call it the conventional polarized-difference dehazing (PD), to better display the details of the image, we display in Fig. 6 the enlarged views of parts of the card and the toy monk. It can be seen that the result of using UDCP has obvious color deviation in the image region. The initial result is that although there is still noise influence in the image, it has better effect than the traditional polarization differential dehazing. Finally, by analyzing the final dehazing effect map of this paper, we can find that the image quality is significantly better than the previous methods.

Additionally, we quantitatively evaluated the above experimental results in terms of Peak Signal to Noise Ratio (PSNR) and Structural Similarity Index (SSIM),see Table 1. The data once again proves the superiority of the method in this paper.

Using the method of this article, we obtained nineteen multi-view dehazing images. We apply the synthetic aperture refocusing algorithm to these nineteen images. This allows us to make a partially occluding foreground object disappear, revealing the object hidden behind it. Fig. 7 demonstrates this idea, using a toy monk behind the plant and a card behind the plant.

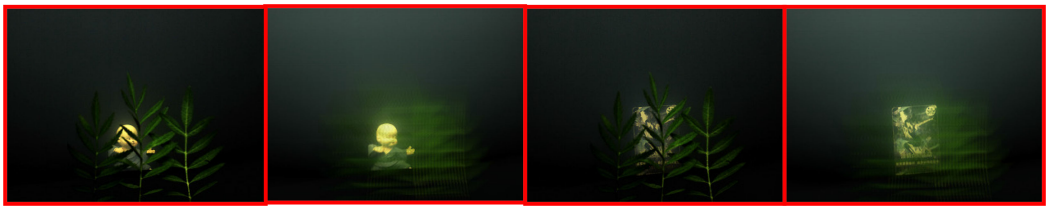

Fig. 7. Synthetic aperture de-occlusion effect diagram.

5. Discussion

Through experiments, we found a method to recover underwater images by obtaining the spatial distribution of the degree of polarization of backscatter and intensity from multi-view images, and proved the feasibility and effectiveness of this method in underwater imaging process. Underwater image dehazing and fog imaging have always been a great challenge in the field of computer vision. This is due to the scattering and attenuation of light due to the existence of scattered particles in water or air, resulting in the loss of effective information in the target scene. Synthetic aperture imaging technology is used to obtain multi-view images of the target scene, which increases the amount of information of the target and can achieve deocclusion. Combined with polarization differential technology, it can effectively eliminate the influence of scattering particles and restore effective information of the target scene.

In order to obtain a polarization difference image, we need to manually rotate the polarizing plate at the front end of the camera, which has certain limitations on real-time dehazing of dynamic scenes. So in the future work, we will focus on solving the above problems. In the future, we will combine the camera array and the polarizer array to reduce the complexity of operation and realize the real-time dehazing of the single shot image of the camera array.

6. Conclusion

In this paper, an underwater image dehazing method based on synthetic aperture imaging and polarization difference imaging is proposed. The degree of polarization of backscatter and the intensity of multi-view images are obtained to retrieve the object radiation, and the dehazing operation of the collected light field image is realized. The expected experimental results are obtained. Future work will focus on improving our experimental model, considering the combination of polarizer arrays and camera arrays to achieve real-time imaging. Finally, we hope to test these methods on more complex scenes where the occlusion environment is more complex and the target depth difference is larger, to find an effective way for light field imaging in underwater image restoration and 3D reconstruction.

References

[1] J. S. Jaffe, “Computer modeling and the design of optimal underwater imaging systems,” *IEEE J. Ocean. Eng.*, vol. 15, no. 2, pp. 101–111, May 1990.
[2] W. Hou, S. Woods, E. Jarosz, W. Goode, and A. Weidemann, “Optical turbulence on underwater image degradation in natural environments,” *Appl. Opt.*, vol. 51, no. 14, pp. 2678–2686, 2012.
[3] G. D. Gilbert and J. C. Pernicka, “Improvement of underwater visibility by reduction of backscatter with a circular polarization technique, ” *Appl. Opt.*, vol. 6, pp. 741–746, 1967.
[4] S. Serikawa and H. Lu, “Underwater image dehazing using joint trilateral filter,” *Comput. Elect. Eng.*, vol. 40 pp. 41–50, 2014.
[5] K. He, J. Sun, and X. Tang, “Single image haze removal using dark channel prior,” *IEEE Trans. Pattern Anal. Mach.Intell.*, vol. 33, no. 2, pp. 2341–2353, Dec. 2011.
[6] Y. Y. Schechner and N. Karpel, “Recovery of underwater visibility and structure by polarization analysis,” *IEEE J. Ocean. Eng.*, vol. 30, no. 3, pp. 570–587, Jul. 2005.
[7] J. Liang, L. Ren, H. Ju, W. Zhang, and E. Qu, “Polarimetric dehazing method for dense haze removal based on distribution analysis of angle of polarization,” *Opt. Exp.*, vol. 23, pp. 26146–26157, 2015.

[8] M. C. Roggemann and B. M. Welsh, *Imaging Through Turbulence*. Boca Raton, FL, USA: CRC Press, 1996.
[9] P. Wang, Q. Chen, G. Gu, W. Qian, and K. Ren, "Polarimetric image discrimination with depolarization mueller matrix," *IEEE Photon. J.*, vol. 8, no. 6, Dec. 2016, Art. no. 6901413.
[10] M. Levoy, B. Chen, and V. Vaish, "Synthetic aperture confocal imaging," *ACM Trans. Graph.*, vol. 23, pp. 825–834, 2004.
[11] C. Fuchs, M. Heinz, and M. Levoy, "Combining confocal imaging and descattering," in *Proc. Eurograph. Symp. Rendering*, 2008, pp. 1245–1253.
[12] E. Trucco and A. T. Olmos-Antillon, "Self-tuning underwater image restoration," *IEEE J. Ocean. Eng.*, vol. 31, pp. 511–519, 2006.
[13] H. Hu, L. Zhao, B. Huang, X. Li, H. Wang, and T. Liu, "Enhancing visibility of polarimetric underwater image by transmittance correction," *IEEE Photon. J.*, vol. 9, no. 3, Jun. 2017, Art. no. 6802310.
[14] Q. Xu *et al.*, "Transmitting characteristics of polarization information under seawater," *Appl. Opt.*, vol. 54, no. 21, pp. 6584–6588, 2015.
[15] H. Hu, L. Zhao, X. Li, H. Wang, and T. Liu, "Underwater image recovery under the nonuniform optical field based on polarimetric imaging," *IEEE Photon. J.*, vol. 10, no. 1, Feb. 2018, Art. no. 6900309.
[16] T. Treibitz and Y. Y. Schechner, "Active polarization descattering," *IEEE Trans. Pattern Anal. Mach. Intell.*, vol. 31, no. 3, pp. 385–399, Mar. 2009.
[17] K. Skinner and M. Johnson-Roberson, "Towards real-time underwater 3D reconstruction with plenoptic cameras," in *Proc. IEEE/RSJ Int. Conf. Intell. Robots Syst.*, 2016, pp. 2014—2021.
[18] K. A. Skinner and M. Johnson-Roberson, "Underwater image dehazing with a light field camera," in *Proc. IEEE Conf. Comput. Vis. Pattern Recog. Workshops*, 2017, pp. 1775–1782.
[19] J. Tian, Z. Murez, T. Cui, and Z. Zhang, "Depth and image restoration from light field in a scattering medium," in *Proc. IEEE Int. Conf. Comput. Vis.*, 2017, pp. 2420–2429.
[20] Y. Y. Schechner, S. G. Narasimhan, and S. K. Nayar, "Polarization-based vision through haze," *Appl. Opt.*, vol. 42, pp. 511–525, 2003.
[21] B. Huang, T. Liu, H. Hu, J. Han, and M. Yu, "Underwater image recovery considering polarization effects of objects," *Opt. Exp.*, vol. 24, pp. 9826–9838, 2016.
[22] W. Ma *et al.*, "Unstructured synthetic aperture photograph based occluded object imaging," in *Proc. IEEE Int. Conf. Image Graph.*, 2013, pp. 34–39.
[23] Zhou *et al.*, "Enhanced reconstruction of partially occluded objects with occlusion removal in synthetic aperture integral imaging," *Chin. Opt. Lett.*, vol. 9, no. 4, pp. 30–33, 2011.